OXFORD CDE

Journal of Computational Design and Engineering, 2024, **11**, 359–373

DOI: 10.1093/jcde/qwae053
Advance access publication date: 13 June 2024
Research Article

AI-powered fire engineering design and smoke flow analysis for complex-shaped buildings

Yanfu Zeng [1], Zhe Zheng[2], Tianhang Zhang[1], Xinyan Huang [1,*] and Xinzheng Lu [2,*]

[1]Department of Building Environment and Energy Engineering, The Hong Kong Polytechnic University, Hong Kong, 999077, China
[2]Department of Civil Engineering, Tsinghua University, Beijing, 100000, China
*Correspondence: xy.huang@polyu.edu.hk (X.H.); luxz@tsinghua.edu.cn (X.L.)

Abstract

This paper aims to automatize the performance-based design of fire engineering and the fire risk assessment of buildings with large open spaces and complex shapes. We first establish a database of high-quality fire simulations for diverse building shapes with heights up to 60 m and complex atriums with volumes up to 22 400 m^3. Then, artificial intelligence (AI) models are trained to predict the soot visibility slices for new fire cases in buildings of different atrium shapes, symmetricities, and volumes. Two deep learning models were demonstrated: the pix2pix generative adversarial network (GAN) and image-prompt diffusion model. Compared with high-fidelity computational fluid dynamics fire modeling, the available safe egress time predicted by both models shows a high accuracy of 92% for random atrium shapes that are not distinct from the training cases, proving their performance in actual design practices. The diffusion model reproduces more flow details of the smoke visibility profiles than GAN, but it takes a longer computational time to render the fire scene. This work demonstrates the potential of leveraging AI technologies in building fire safety design, offering significant cost and time reductions and optimal solution identification.

Keywords: intelligent design, deep learning, smart firefighting, atrium fire safety, fire engineering, ASET

Abbreviations

AI:	Artificial intelligence
ASET:	Available safe egress time
CFD:	Computational fluid dynamics
GAN:	Generative adversarial networks
HRR:	Heat release rate
PBD:	Performance-based design

1. Introduction

The rapid global urbanization and the emergence of new construction materials and technologies have led to a significant increase in the number of constructed buildings and infrastructures in recent decades. These designs are becoming larger, taller, deeper, and more complex (Fig. 1). For instance, the newly constructed Baiyun high-speed railway station in Guangzhou has a fire compartment area of over 70 000 m^2, which is seven times more than the maximum value regulated by the fire code (China Railway Third Survey & Design Institute Group, 2016). These advancements pose challenges to current fire regulations, necessitating the adoption of performance-based design (PBD) solutions with supporting analysis to address non-compliant design issues.

In PBD practices, the fire-smoke dynamics under proposed design provisions shall be predicted and analyzed. Although past researchers have developed many semi-empirical correlations for engineering practices, such as Alpert's ceiling jet correlations (Alpert, 1972), Kawagoe's Law (Kawagoe & Sekine, 1963), and Heskestad's fire plume model (Heskestad, 1984), these equations are derived from the simplistic experimental scenarios and may exhibit discrepancies when applied to buildings with complex geometries (Luo *et al.*, 2024; Wang *et al.*, 2024; Zeng, Wong, *et al.*, 2023). With the rapid development of numerical simulation methods, fire modeling based on computational fluid dynamics (CFD) software has become widely adopted in fire engineering designs (Wong & Wu, 2024; Zeng, Wong, *et al.*, 2019; Zheng *et al.*, 2022).

CFD modeling can simulate the detailed process of fire-induced smoke spreading, and its accuracy has been verified (McGrattan *et al.*, 2023) and validated (McGrattan *et al.*, 2021) by numerous studies. With the modeling results, engineers can assess the effectiveness of the fire compartmentation, smoke barrier, smoke ventilation system, and other design features. Ideally, it can help to identify the most cost-effective design solutions, such as determining the minimum smoke extraction capacity required to maintain the pre-defined smoke clearance height. However, due to its time-consuming nature, the CFD-based smoke behavior analysis is very costly, and optimal design solutions cannot be identified without a substantial amount of resources (Zeng & Huang, 2024b). Moreover, the summarized experiences and insights from the past designs are often limited to individual levels and cannot be effectively shared and applied by others or the entire industry.

Given these challenges, there is a pressing need for intelligent transformation in design methods. Artificial intelligence (AI), particularly deep learning networks, has emerged as a promising solution to address the aforementioned issues. Deep learning networks can leverage historical data to learn hidden patterns and make accurate predictions quickly (Zeng & Huang, 2024a). It has

Received: April 6, 2024. **Revised:** May 27, 2024. **Accepted:** May 29, 2024

Figure 1: Innovative modern buildings with large-volume and complex spatial design.

been extensively studied for various design tasks in the architecture, engineering, and construction industry in recent years. For example, Isola *et al.* (2017) first proposed a pix2pix architecture based on generative adversarial networks (GANs), which can generate façade design by providing a building framework. Huang and Zheng (2018) trained an AI engine capable of designing interior layouts based on architectural room plans. Today, deep learning algorithms have also been widely applied to building structural designs (Liao *et al.*, 2024), such as shear wall allocation (Liao *et al.*, 2021, 2022, 2023; Lu *et al.*, 2022; Zhao, Fei, *et al.*, 2023; Zhao, Liao, *et al.*, 2023b), structural beam layout (Zhao, Liao, *et al.*, 2022, 2023a, 2024), tube framework design (Fei, Liao, Huang, *et al.*, 2022), wall size calculation (Feng *et al.*, 2023), digital interpretation of design codes (Zheng *et al.*, 2022, 2024), and estimation of material consumption (Fei, Liao, Lu, *et al.*, 2024). Research has shown that AI can provide engineering designs comparable with engineers, while the efficiency could be 20 times higher (Liao *et al.*, 2021).

In the realm of building fire safety engineering, AI has demonstrated its ability to accurately predict fire behavior and characteristics, such as heat release rate (HRR, Wang *et al.*, 2022, 2023), flashover occurrence (Tam *et al.*, 2022; T. Zhang, Wang, Wong, *et al.*, 2022), fire location (Wu, Park, *et al.*, 2021; Zhang, Wang, Zeng, *et al.*, 2022), temperature field (Wu, Zhang, *et al.*, 2022; Zhang *et al.*, 2022), and fire-induced heat transfer (Bakas & Kontoleon, 2021). AI can also predict the performance of construction material under fire exposure with less computational cost (Nguyen *et al.*, 2021). As for the design automation, Su *et al.* (2021) first used AI to predict the smoke movement for the atrium with proposed design parameters, such as building height and HRR of design fire, with comparable results with CFD modeling while the computational time of within 1 s. Afterwards, Zeng, Zhang, *et al.* (2022) encoded the AI model into an open-access software (IFETool) for fire safety design analysis and provided a quick assessment of the available safe egress time (ASET) for simplistic box-shaped atrium. More recently, we have developed a GAN-based AI model that achieved quick prediction of temperature field and fire-detection time for buildings with complex two-dimensional (2D) floor plans with an accuracy of 88% (Zeng, Li, *et al.*, 2023). With AI methods, the industry can benefit from significant reductions in cost, time, and computational demands (Bakas & Kontoleon, 2023).

This work aims to upgrade our previous AI model to handle the buildings and atrium spaces with complex 3D shapes so that AI-assisted design can be adopted in more realistic fire engineering design practices. A numerical database containing high-fidelity fire simulations with different atrium geometries is first established, which is then used to train deep learning models constructed with (i) pix2pix GAN and (ii) image-prompt diffusion model. After the training, both AI models are used to predict the smoke movement for new buildings, and their results are compared with CFD modeling to demonstrate their efficiency and accuracy.

2. AI Model Construction

2.1. Database preparation

This study aims to develop an AI-driven automatic fire-engineering design tool for an atrium (or large-open space) because it is the most common and representative space in building fire safety analysis and PBD practices. Atriums are characterized by large, connected spaces with ceiling heights typically exceeding 10 m. They are commonly found in various types of projects, including stadiums, terminals, shopping malls, convention halls, and more. Given their significance, atriums were selected as the focus of this study, and a dedicated atrium fire database was created using CFD simulations conducted with Fire Dynamics Simulator version 6.7.7 (McGrattan *et al.*, 2019). By referring to some famous realistic buildings, 26 different atrium schemes were constructed with various degrees of geometry complexity, as shown in Fig. 2.

To expand the diversity of the database, each scheme has two sub-cases, wherein at least one design parameter is different, such as the fire location, atrium height, width, symmetricity, and complexity. Examples of database expansion are shown in Fig. A1.

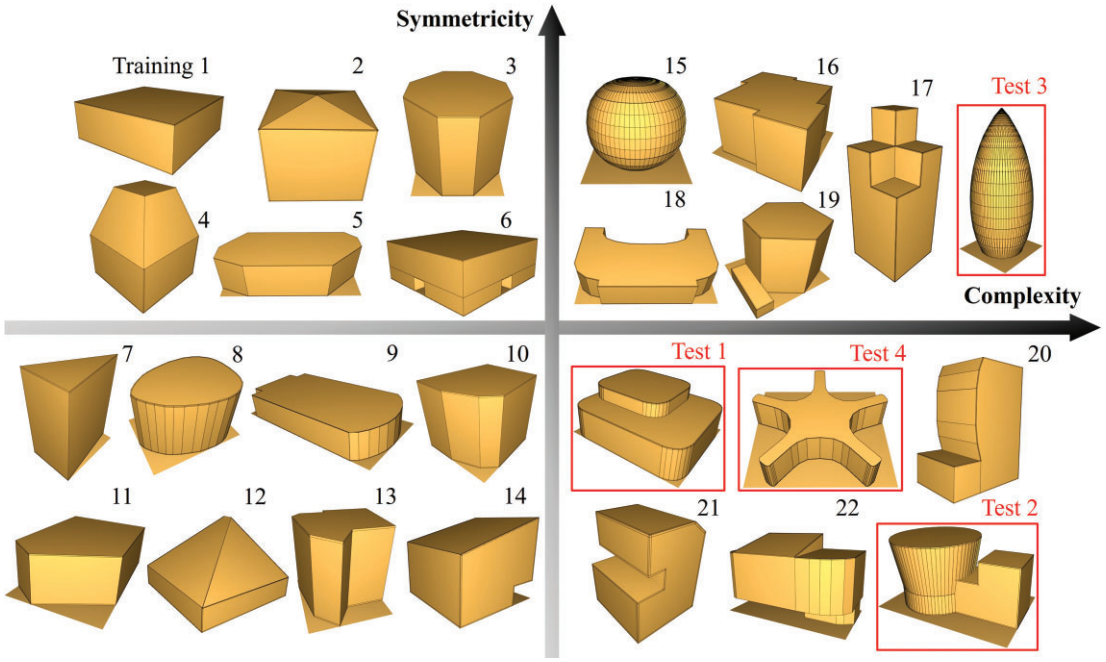

Figure 2: CFD database containing atriums with different levels of symmetricity and complexity.

In total, 52 fire scenarios were simulated to form the atrium fire database. Table 1 provides an overview of the dimensional distribution of the atrium domains in the training dataset. Sub-cases are also presented in this table. For example, 7A/7B means this scheme has sub-cases with the same atrium shape while different dimensions. Other schemes have sub-cases with different fire locations, e.g., one fire is located in the middle and another fire is located closer to the side wall.

The length and width of the atriums ranged from 10 to 60 m, while the atrium height spanned from 10 to 50 m. The atrium volume varied from 820 to 22 400 m^3. It should be noted that the computational domain volume will be larger than the volume of the atrium. This is because the computational domain for all simulations was set as a rectangular shape for convenient data processing and AI training, while the irregular shape of the atriums results in some parts of the computational domain being outdoor spaces.

The turbulence model utilized in this study was the Large Eddy Simulation method. For all simulations, a *t*-square (t^2) growth fire was adopted, which is commonly used in design practices to represent the burning of different fuels. For simplicity, the fire HRR was set to reach a peak value of 1000 kW at 150 s, with a fast growth rate, and remained constant until 1200 s. It should be noted that, in PBD practices, the adopted peak HRR is generally higher than the value of 1 MW, depending on the type and distribution of fuel. The reason for adopting a relatively small fire is to reduce the database preparation time, because the focus of this research is to predict smoke flow in complex-shaped buildings, as well as, the feasibility of using different deep learning models. The fuel used was polymethyl methacrylate (PMMA), and its properties were set to the default values provided by the SFPE Handbook (Khan *et al.*, 2016). The area of the fuel bed was 1.92 m^2, resulting in an HRR per unit area of 520 kW/m^2. The ambient temperature was set at 20°C.

2D slices of soot visibility were set at X, Y, and Z directions to record the smoke movement process. In X and Y directions, two slices were positioned across the center of the fuel bed. The Z slice was located at 2 m above the fuel bed, as it is a typical criterion for smoke clearance height in design standards (Australian Building Codes Board, 2022; Building Department, 2011; New Zealand Centre for Advanced Engineering, 2008). These slices provide valuable information about the smoke dispersion process and will serve as the target outputs for the AI model.

Grid resolution is an important parameter in CFD simulation to ensure numerical accuracy. A sensitivity study was performed in an atrium with 20 × 20 × 20 m^3 to determine an appropriate grid size that balances simulation accuracy and computational resources. To conserve computational resources, steady-burning fires were simulated, with the HRR reaching 1 MW once the simulation started. As shown in Fig. A2, reducing the grid size from 0.2 to 0.1 m did not yield significant improvements in the simulation results, while the computational time can be saved by 72% for the 0.2-m cell case. Therefore, a cell size of 0.2 m was applied for all the fire simulations to speed up the computational process while maintaining accuracy. The total number of cells ranged from 125 000 to 3000 000, depending on the volume of the computational domain (see Table 1). The simulations were run with parallel computing (32 cores), and the average computational time was approximately 30 h, with a maximum value of 91 h for Training case 20.

To validate the proposed computational settings, a reproduction of an atrium fire experiment (Ayala *et al.*, 2016) was performed. Fig. A3 compares the measured temperature by thermocouples with the predicted temperature by CFD modeling at different heights and axes. It can be seen that the simulation results with proposed settings agree well with the experimental records, with an average discrepancy of approximately 11%. This confirms the fidelity of the CFD modeling and ensures that the data quality for training the AI model is satisfactory in terms of the conventional PBD standard.

2.2. Fire-scene data pre-processing

The inputs of the deep learning model should be defined as the parameters that greatly influence the outputs. As the main

Table 1: Dimension distribution of the atrium in the database (see examples in Fig. A1 in Appendix 1).

Dataset	Case no.	Length ($\vec{x}$; m)	Width ($\vec{y}$; m)	Height ($\vec{z}$; m)	Atrium volume (m^3)	Cell no.
Training	1	40	40	14	22 400	2800 000
	2	20	20	20	7280	1000 000
	3	15	15	15	2625	421 875
	4	16	16	20	3733	640 000
	5	50	20	14	12 200	1750 000
	6	40	40	15	23 040	3000 000
	7A/7B	10/15	15/15	20/20	1500/2300	375 000/562 500
	8A/8B	13/18	24/24	10/15	3120/6480	390 000/810 000
	9	60	30	10	16 380	2250 000
	10	15	15	15	2625	421 875
	11	30	20	10	5390	750 000
	12	30	30	20	13 778	2250 000
	13A/13B	10/10	10/10	10/20	820/1640	125 000/250 000
	14A/14B	20/20	20/30	25/18	5472/8088	900 000/1350 000
	15	20	20	17	3560	850 000
	16	25	25	15	7695	1171 875
	17	20	20	50	16 000	250 000
	18	50	30	10	10 940	1875 000
	19	24	28	20	8580	1680 000
	20	30	20	40	18 400	3000 000
	21A/21B	10/16	10/10	13/13	1125/1868	162 500/260 000
	22	20	40	25	12 758	1680 000
Testing	1A/1B	35/15	35/15	13/25	10 405/4005	1706 250/703 125
	2	30	20	15	4522	1125 000
	3A/3B	18/10	18/10	41/21	6620/912	1660 500/262 500
	4A/4B	42/25	40/25	10/10	4910/4910	2100 000/781 250

targeted attribute of this study, the building shape needs to be first considered. For model training purposes, all input and output information need to be processed in the form of numbers or matrices. The information on building shape can be fully encoded in a 3D matrix. In this matrix, cells with wall existence were encoded with a value of 1, while all other cells were set to 0. By doing that, the building shape can be numerically reproduced. All the building shape matrices should also be resized to the same size so that they can be stacked together, and the uniform dimension of 128 × 128 × 128 was adopted as the balanced value. Ideally, these 3D matrices could be directly used as inputs to train the model, allowing the building spatial information to be fully preserved for the AI to learn. However, this approach requires massive computational resources that exceed the capacity of current graphics processing unit (GPU) with a memory of 16GB.

As an alternative data processing approach, six projection matrices were used to capture the spatial information, as depicted in Fig. 3. Since the computational domains are all cuboid-shaped, there are six faces corresponding to the X-positive, X-negative, Y-positive, Y-negative, Z-positive, and Z-negative directions, respectively. A matrix was generated for each face, where the values represent the relative distance between the face and the exterior wall. For example, a value of 0% indicates that the wall is adjacent to the face at that specific point, a value of 50% means the wall is located in the middle of the face, and a value of 100% suggests that there is no wall present at that point. These six projection matrices collectively encompass the spatial information of the building and, when combined, can effectively reproduce the shape of the atrium in a comprehensive manner.

In Section 2.1, it was mentioned that the X and Y slices of visibility across the fuel bed, as well as the Z slice at 2 m above the fuel (or the fire source), are the desired outputs of the AI model. In addition to the six projection matrices, three additional mask matrices were generated as inputs for the AI model. These mask matrices are paired with the output matrices and encode information about the indoor area, wall boundaries, and outdoor area as 0, 0.5, and 1, respectively. They serve as filters during the training process, guiding the AI model to understand which areas are more likely to have smoke and which areas are not. Furthermore, lines encoded with 0.3 are added in the mask slices to store the fire position.

While the distance information stored in projection matrices is relative and all the matrices are resized to 128 × 128, the information on original building dimension should also be given in terms of length, width, and height. Moreover, the post-ignition time shall be informed since the smoke flows with time. As a result, the final size of input matrix is then 128 × 128 × 13, while the 13 channels consist of six channels for the building projection matrices to store the shape information, three channels for mask matrices to outline the smoke spreading area and indicate the fire location, three channels to tell the building dimension, and one channel to specify the post-ignition time. The output matrix is correspondingly 128 × 128 × 3, representing the soot visibility slices from X, Y, and Z directions under the specific timestep.

To ensure a robust evaluation of the proposed generative model, the database is divided into training and testing datasets. The training dataset, which accounts for 85% of the total data (Fig. 2), is used to enable the model to learn the correlations and patterns between the designed inputs and smoke outputs. On the other hand, the testing dataset, constituting the remaining 15%, serves as an independent dataset that assesses the final performance and generalization ability of the trained model. This separation allows for an unbiased evaluation of the model's effectiveness on new, unseen data.

To further enrich the learning data, the training dataset is augmented by rotating the atriums at angles of 90°, 180°, and 270°.

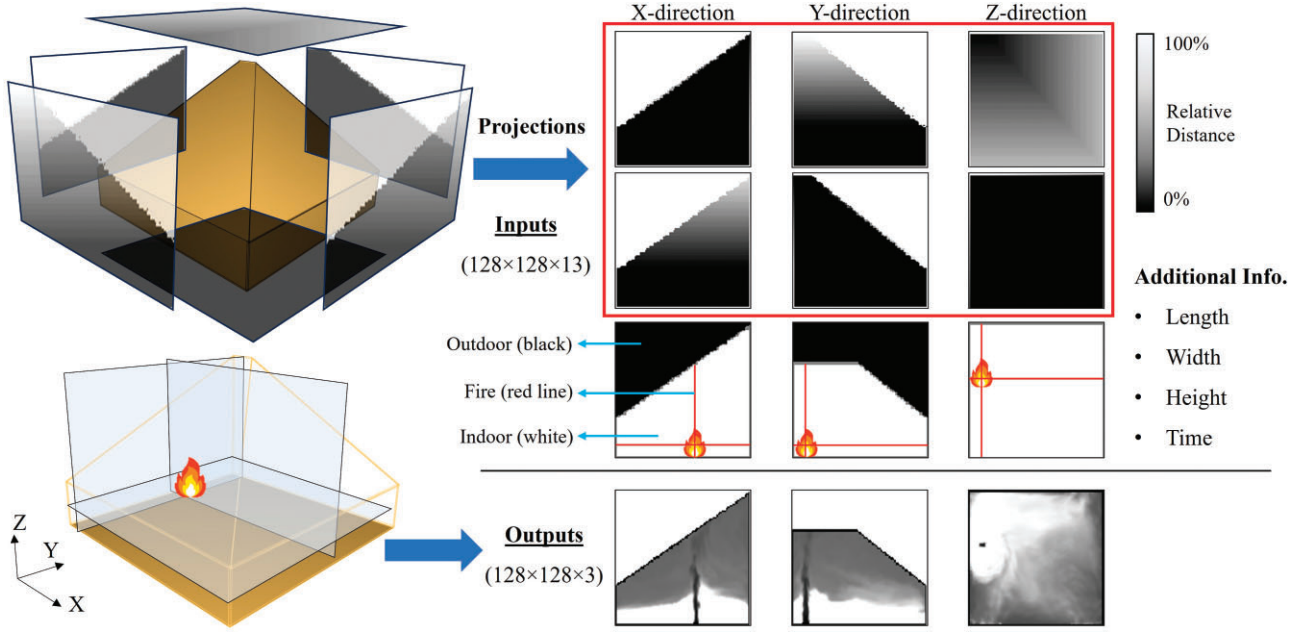

Figure 3: Data process of AI model inputs and outputs.

Consequently, the number of data samples is tripled. Each case initially consists of 60 data samples, considering a simulation time of 1200 s with a data extraction interval of 20 s. As a result of the augmentation, the total number of data samples in the training dataset reaches 10 560, providing a larger and more diverse dataset for the model to learn from.

2.3. AI architectures

Inspired by the previous work (Zeng, Li, *et al.*, 2023), a deep learning model based on GAN with architecture of pix2pix (Isola *et al.*, 2017) is firstly constructed. Specifically, pix2pix GAN model consists of a generator and discriminator, while the detailed architecture is depicted in Fig. 4a. The generator is established by following the U-Net structure, which is responsible for generating fake visibility slices that can deceive the discriminator. The discriminator, on the other hand, distinguishes whether the generated outputs are real or synthetic, thereby improving the performance of generator.

In the generator, the input matrix undergoes seven convolution operations to extract corresponding features. The activation function in the convolutional layers is ReLU, and the padding mode is set to same. The size of the convolutional kernels is 4 × 4, and both the pooling and upsampling have a size of 2 × 2. To ensure that the model has good generalization to meet different design requirements, neurons in the neural network are randomly dropped with a probability of 0.2 after each upsampling operation. The activation function in the output layer is tanh. The generated images from the generator are mixed with real images and fed into the discriminator together with the input matrix. The discriminator undergoes multiple pooling operations to condense the information into a 16 × 16 output feature map and determines whether the image is real or generated.

The mean absolute error, defined as the difference between the CFD simulations and AI predictions, was adopted as the loss function of the generator, which can be minimized through the number of training iterations. The loss function of discriminator was defined as *binary_crossentropy*, as it provides a binary judgment of the result fidelity.

A recent study also shows that the diffusion model might have a better performance in the field of generative structure design (Gu *et al.*, 2024). Therefore, a deep learning model based on an image-prompt diffusion model was constructed as well (Fig. 4b). The diffusion model consists of forward diffusion and reverse denoising processes. The forward diffusion process is a Markov process where Gaussian noise is added at each step (Ho *et al.*, 2020), and the reverse denoising process is used to recover the target image from noise, where neural networks are used to predict noise at each step.

The U-Net with temporal encoding (Dhariwal & Nichol, 2021) was used as the denoising model. The utilized U-Net architecture is shown in Fig. 4b. H1, H2, H3, and H4 represent the channel numbers of the intermediate blocks in the U-Net. Specifically, the values of H1 and H2 are 64 and 128, respectively. H3 can be either 192 or 256; H4 can be 256 or 512 (Gu *et al.*, 2024). Besides, to ensure a good model generalization, neurons in the neural network are randomly dropped with a probability of 0.2. The mean squared error loss, defined as the difference between the true noise added and the noise via AI predictions, was adopted as the loss function of the denoising model.

3. Results and Discussion

This section focuses on presenting the predictions of pre-trained AI models for four testing cases with varying levels of geometry complexity. The objective is to investigate the limitations of the AI model's prediction capability. Videos S1–S4 provide a visual comparison of the evolving soot visibility between CFD modeling and AI models throughout the entire 1200-s simulation time for each case. These videos offer a comprehensive illustration of how well the AI model captures the dynamics of soot visibility in comparison to the more computationally intensive CFD simulations.

3.1. Smoke flow pattern and visibility

Figure 5 showcases the generated figures at different timesteps for Test 1A, which has a domain size of 30 × 35 × 13 m^3 (see

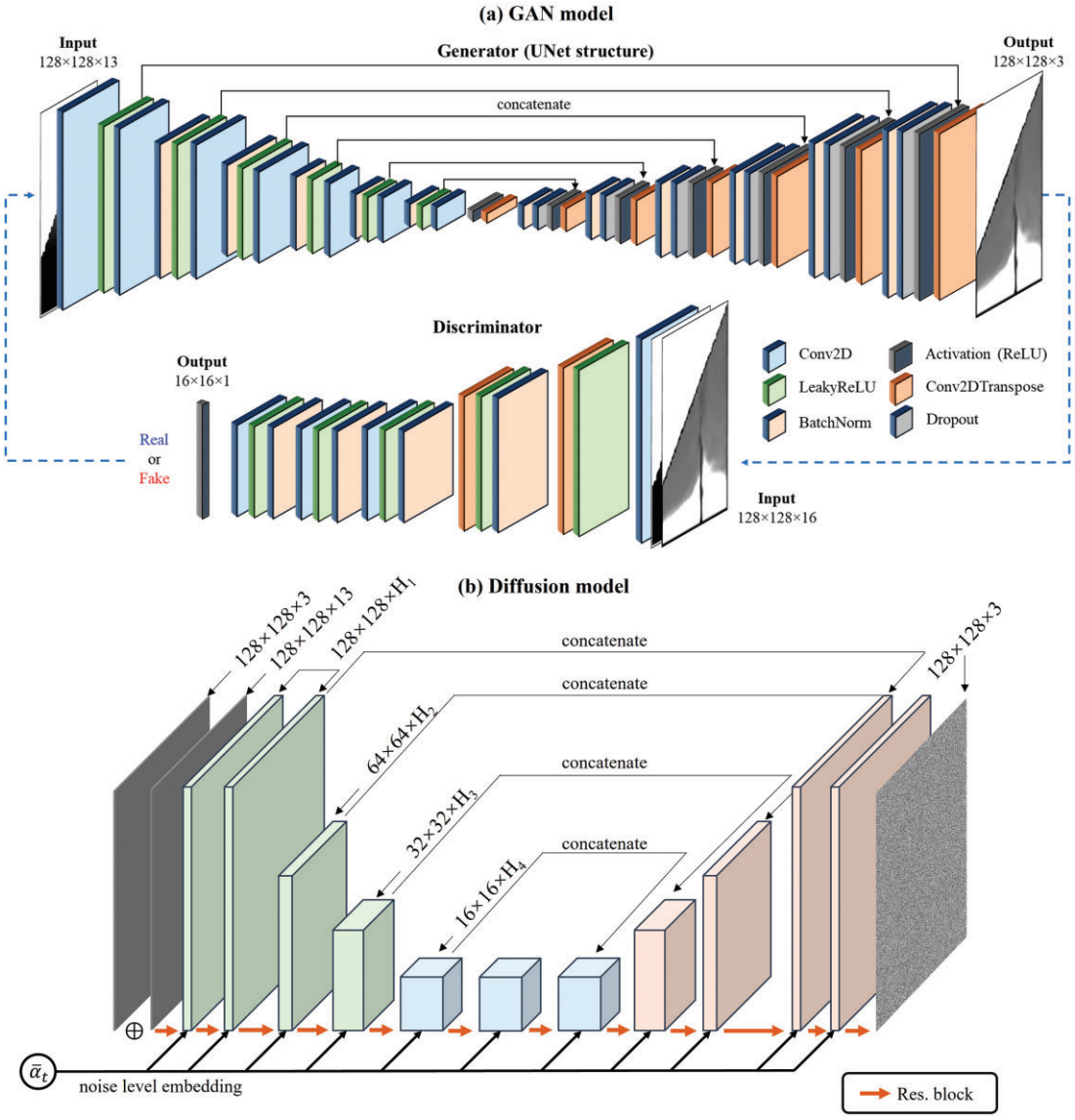

Figure 4: Architecture of deep learning algorithms: (a) pix2pix GAN model and (b) diffusion model.

more detailed comparison in Video S1). The CFD-generated images are outlined in black solid lines, GAN-generated images in blue dashed lines, and diffusion model images in red solid lines. This case presents a scheme with a larger box-shaped space at a lower height and a smaller volume at a higher space. Importantly, this scheme is a completely new case that both AI models had never encountered during the training process. Nevertheless, it is evident that AI models have effectively learned most of the smoke movement patterns from the training data, especially for the diffusion model, and then, applied them to this new case. The fire plumes are accurately identified in the X and Y slices, and the AI successfully reproduces the descending form of the smoke layer from the ceiling to the floor. In the Z slices, the visibility consistently decreases first near the walls and progressively fills the central area, as the smoke tends to flow along the walls faster during its downward movement. Both AI models have also effectively captured this feature.

There are also some local patterns, such as the air entrainment around the fire plume, that are missed by the GAN model. When the high-temperature fire plume rises, it continues to entrain the surrounding air, creating an upward airflow around the plume, which results in a clear area nearby. This phenomenon is influenced by various factors, including air makeup distributions, building size, and fire size, so it is more difficult for the AI model to capture. The turbulent eddies are also ignored by the GAN model. Nevertheless, the diffusion model has shown its powerful learning capability with the successful reproduction of most local patterns. Overall, the GAN model provides a mean relative error of 13.3%, while the value for the diffusion model is 12.6%.

It should be noted, however, that these local smoke behaviors are typically less significant during the fire engineering design process, where the primary focus is on the formation of the smoke layer and its descent speed. By ignoring the details of flow, the GAN model is able to generate all the smoke diagrams for the 20-min fire development in a matter of seconds with a central processing unit (CPU) of 8-core AMD Ryzen 7 5800H 3.20 GHz. In contrast, the diffusion model requires approximately 20 min to generate these images in a server with GPU NVIDIA GeForce RTX 3090 and will take more time to do so by using a personal computer. Therefore, from the design perspective, the diffusion model is not necessarily

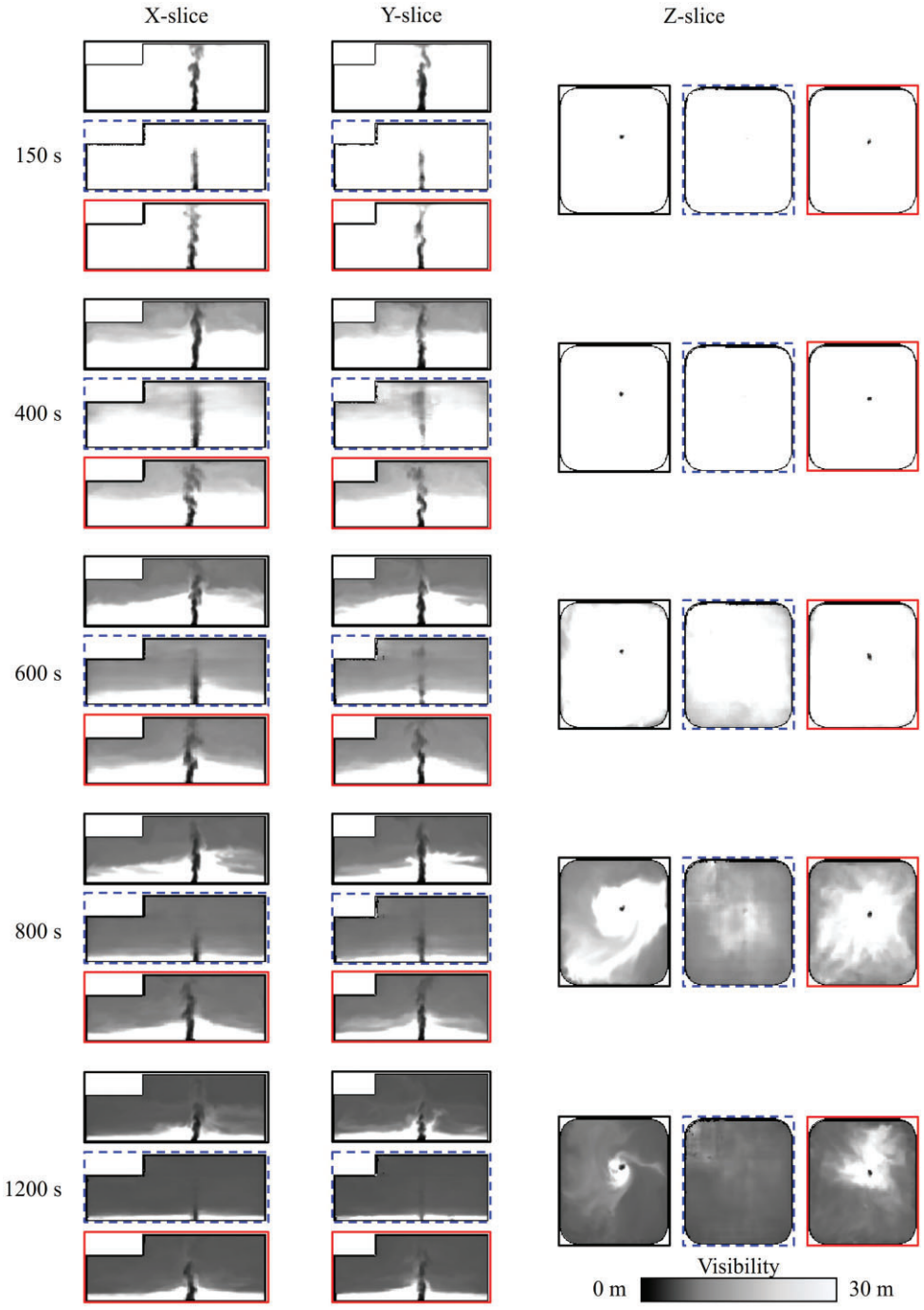

Figure 5: Comparisons of actual (CFD) and predicted (AIs) visibility slices at different timesteps for Test 1A, where the subfigures with black solid outlines are CFD results, blue dash outlines are GAN results, and red solid outlines are Diffusion results (see more detailed in Video S1).

to be the best choice. Nevertheless, it still overperforms the traditional CFD modeling, which takes a few days to get the smoke layer results.

3.2. ASET prediction by AI models

To evaluate the proposed design, engineers need to assess the reach of tenability limits based on predictions of smoke movement. Typically, a smoke clear height of 2 m is adopted (Building Department, 2011). Figure 6a compares the descending profiles of visibility at a height of 2 m for Test 1A, and the smoke figures at 1200 s are also presented in the plots. For the X and Y slices, the average visibility is calculated at a height of 2 m within a 1-m proximity to the side walls, as smoke tends to descend along the walls. In the Z slice, the visibility at a height of 2 m is determined by the minimum value that covers over 5% of the area. For instance, if the visibility in more than 5% of the area drops below 20 m, the visibility is recorded as 20 m at that specific timestep. The zone below 10-m visibility is marked in red on the plot, as a visibility of 10 m is commonly used as the tenability limit to determine the ASET. Once the visibility drops below 10 m, the building is considered an unsafe environment for evacuation.

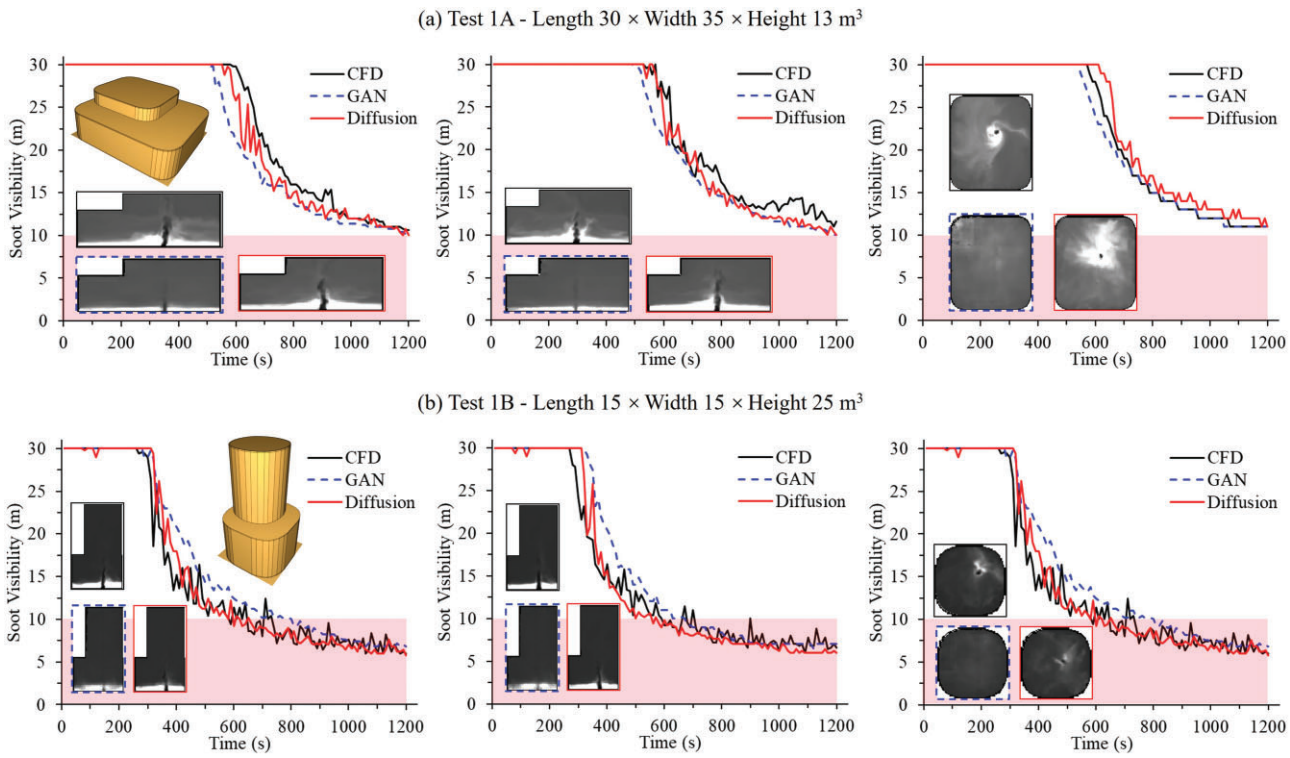

Figure 6: Comparisons of visibility descending profiles at 2-m height for Test 1 with different dimensions.

As depicted in Fig. 6a, both AI models have provided highly accurate smoke descending profiles, with errors of less than 5.2% for the GAN model and 4.7% for the diffusion model. Figure 6b shows the results of Test 1B, a variation of Test 1A with modified length and height. With a higher atrium height and smaller building volume, larger smoke fluctuation can be found in this scheme. Nevertheless, AI predictions still remain comparable with the CFD modeling, with discrepancies of less than 13.6% for the GAN model and 9.8% for the diffusion model. This demonstrates the good generalization capability of the proposed AI models.

Figure 7 displays the visibility profiles for Test 2 (see Video S2), which has a domain size of 30 × 20 × 15 m^3. Test 2 consists of two separate spaces connected by a central corridor, making it a more complex space compared with previous schemes. Still, the AI models can provide accurate predictions for both fire locations on the right side and at the central bottleneck, with discrepancies of less than 8.8%.

In current PBD practices, engineers are responsible for determining typical or dangerous fire locations for assessment based on their expertise and experience, which may introduce biases and uncertainties. Additionally, the high computational resources required for PBD often limit the number of assessed fire locations to only three to six. With AI tools, engineers can now assess more potential fire locations for their projects and identify the worst-case scenarios, ensuring that the design boundaries are fully understood. This eliminates the limitations imposed by computational resource constraints and allows engineers to comprehensively evaluate fire scenarios.

Figure 8a illustrates the results for Test 3A (Video S3), which has a domain size of 18 × 18 × 41 m^3. The AI-generated images still bear similarities to the simulated ones, with a discrepancy of 14.0% for GAN model and 12.8% for diffusion model. However, there is a slight deviation in the smoke layer height between the GAN and CFD predictions, leading to a noticeable discrepancy in the visibility profiles at a height of 2 m for the X and Y slices. One potential cause for this discrepancy is that the majority of our training data has a height ranging from 10 to 30 m, while only 9% of the data covers heights over 30 m (see Table 1). Nevertheless, the GAN model maintains accurate predictions for Z slice with a discrepancy of 8.0%. On the other hand, the diffusion model once again demonstrates its excellent learning capability through accurate predictions of smoke layer height, while the average error is 8.9% for three directions.

To further resolve the concerns caused by the size of numerical database, a scaled-down version of the same atrium shape, Test 3B, was constructed. In this case, the GAN model gives super accurate predictions for the soot visibility profiles, as depicted in Fig. 8b. This confirms the aforementioned concern and highlights the importance of incorporating data diversity in the training process.

To explore the limits/boundaries of the AI prediction, a uniquely shaped atrium (Test 4A) was constructed, which differed significantly from all the training cases. As expected, AI predictions demonstrate significant delays in the descent of the smoke layer, as shown in Fig. 9a (Video S4). Test 4A has a large computational domain of 42 × 40 × 10 m^3, but the majority of this 3D space consists of outdoor areas, with only approximately 30% being within the building. The lack of training data for such outdoor-dominant conditions could be the potential reason that AI model overestimates the internal space of the building and provides relatively slow smoke descent curves, while further verification is required in future work.

To address such an issue, an alternative solution could be to convert the building into a simpler-shaped geometry with an equivalent volume. Test 4B, shown in Fig. 9b, has the same

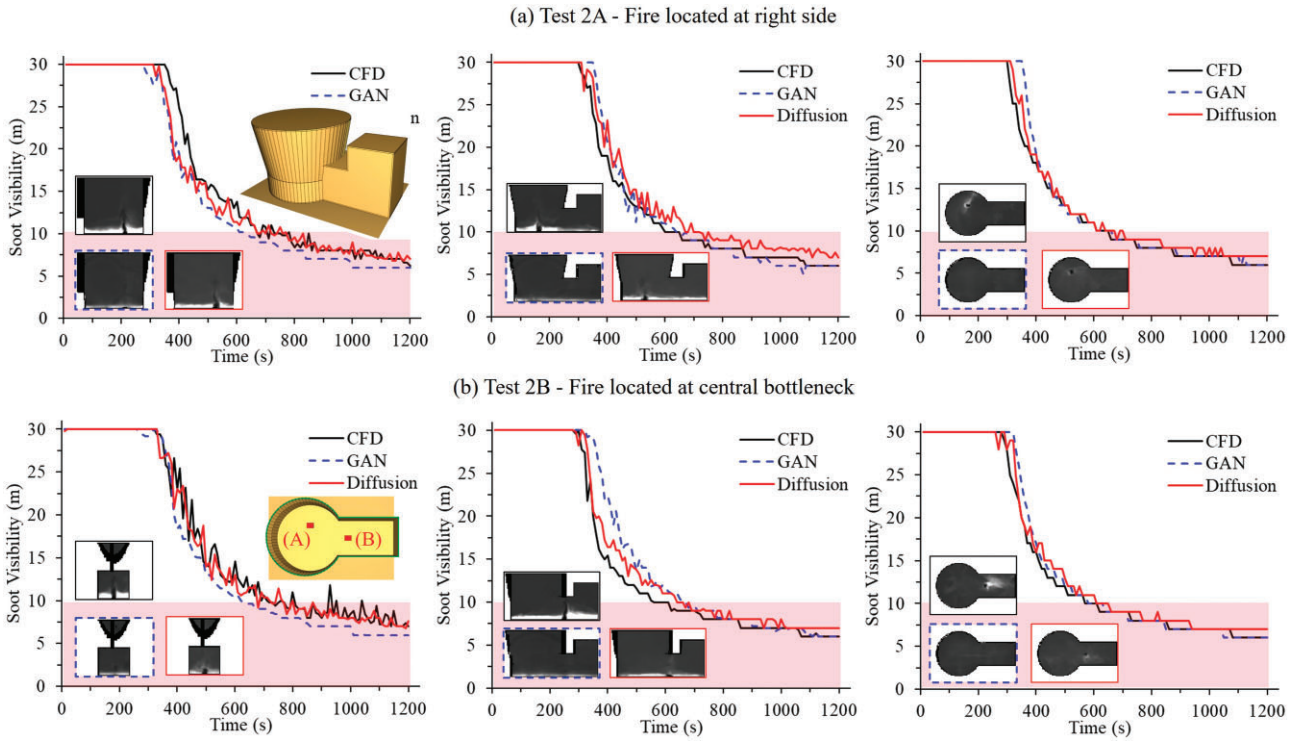

Figure 7: Visibility descending profiles at 2-m height for Test 2 with different fire locations (see Video S2).

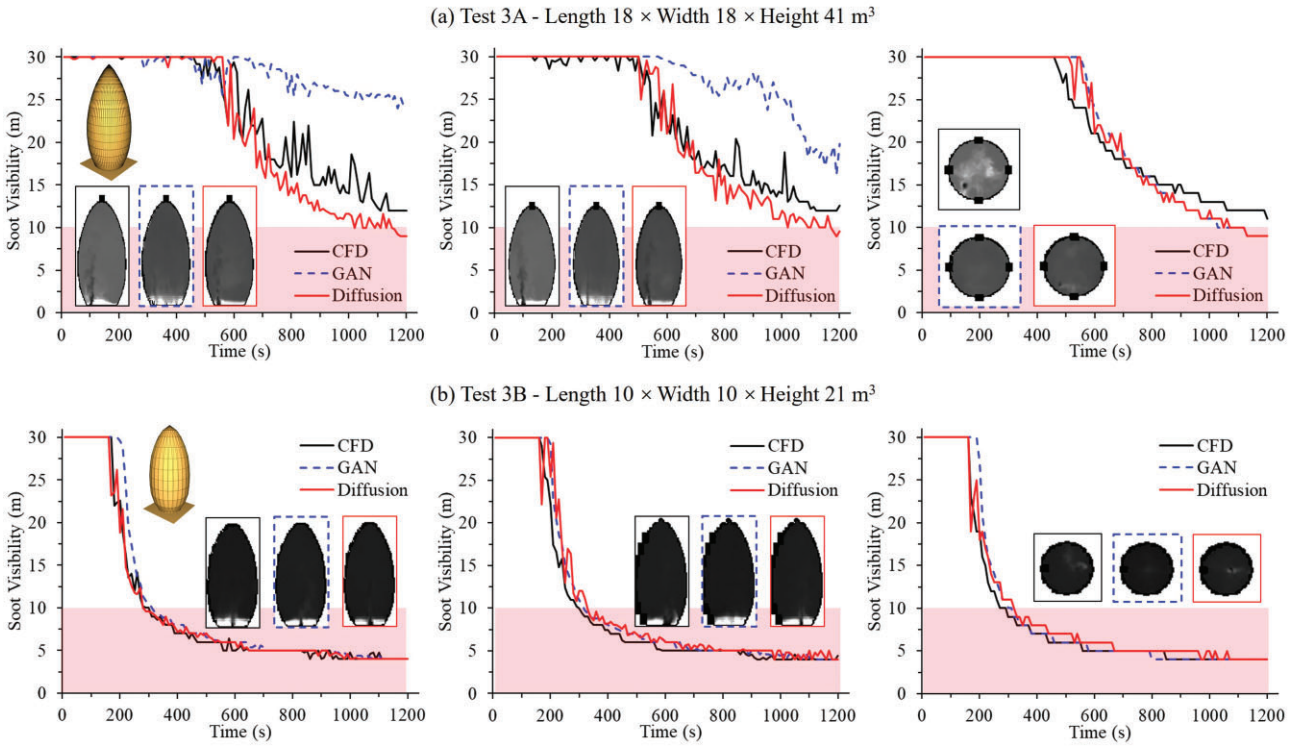

Figure 8: Comparisons of visibility descending profiles for Test 3 with different scales (see Video S3).

indoor floor area as Test 4A but with a cylinder shape. CFD results indicate that these two cases with the same volume exhibit very similar visibility profiles (solid and dashed lines in black). This suggests that the cross-section shape may have minimal impact on smoke layer formation in such a large-volume space, especially when the flaming fire generates a strong smoke plume. Furthermore, AI can easily predict smoke movement in the simpler-shaped space, providing a reference for the complex case. By using this volume-equivalent method, smoke descending profiles with an accuracy of 92.0% can be obtained for Test 4A.

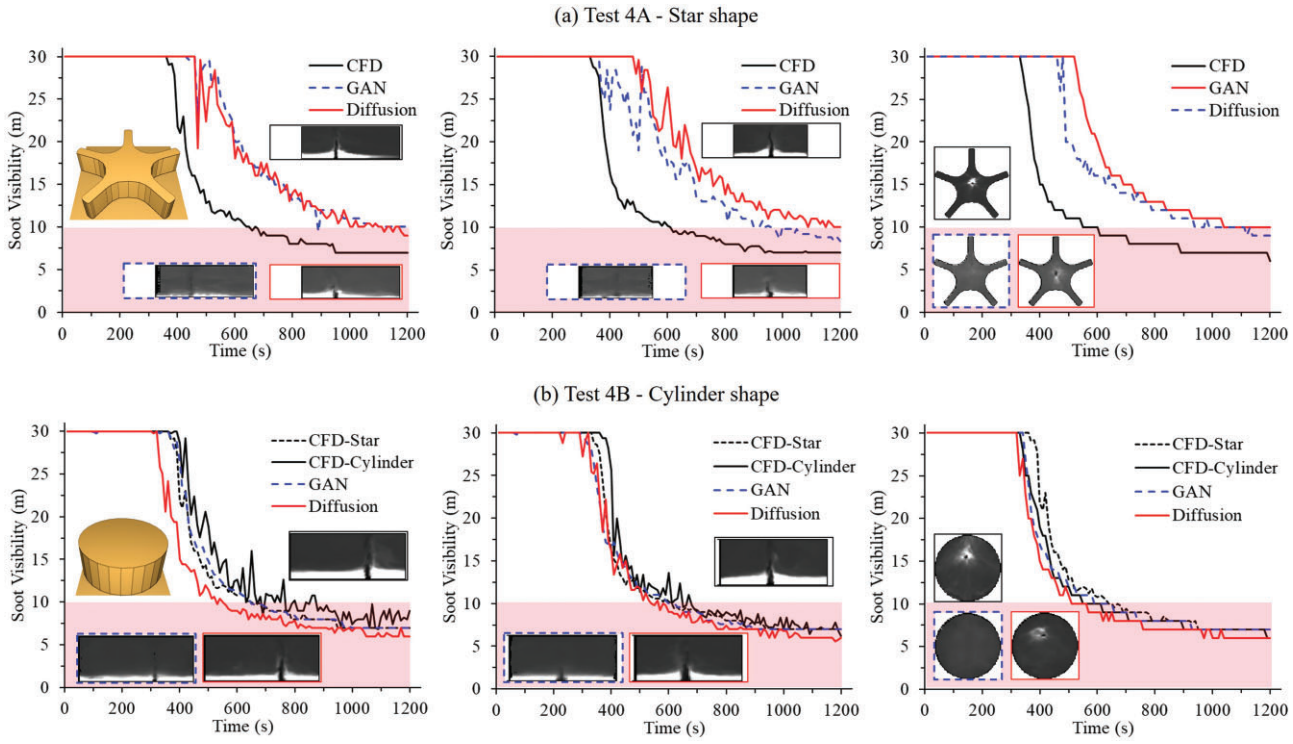

Figure 9: Comparisons of visibility descending profiles for Test 4, where 4A and 4B have the same space volume while different shapes (see Video S4).

It is important to note that this volume-equivalent approach may not always yield accurate results due to the sensitivity of smoke layer development to various factors, such as the features of ventilation and burning fuel (Cheung *et al.*, 2023). However, it can still offer a preliminary evaluation of the proposed design during the early stages of scheme design, where detailed analysis may not be feasible. It also emphasizes that performance of AI model is limited by the feature, size and boundary of the training database. Therefore, cautions must be made before using the model results in practical projects. It is suggested that the size of database shall be further expanded to include more atrium shapes, and the user shall first check if the targeted building is similar to the training cases. While AI tools can help to quickly identify critical conditions, safety margin and CFD verification are still preferred to safeguard the proposed design.

3.3. Impact of AI model on fire engineering design

Based on the visibility descending profiles presented in Figs 6–9, the ASET for each testing case and each direction can be obtained, i.e., the time when visibility drops to 10 m and below. Figure 10 compares the defined ASETs for all testing cases, and it can be seen that most of the results fall within the 20% error range except for Test 4A. The average accuracy can reach over 90% by excluding this distinct case. These results are generated by the GAN model within a few seconds, representing a significant improvement in design efficiency. Although the diffusion model takes a longer time (about 20 min) to render results, more smoke flow details can be reproduced, especially in the case with relatively little learning data. Additionally, this approach allows designers to review multiple potential schemes at early design stages and identify the optimal solutions. Most importantly, the AI approach facilitates sustainable development in terms of fire data and design experience. Previous designs from engineering consulting firms

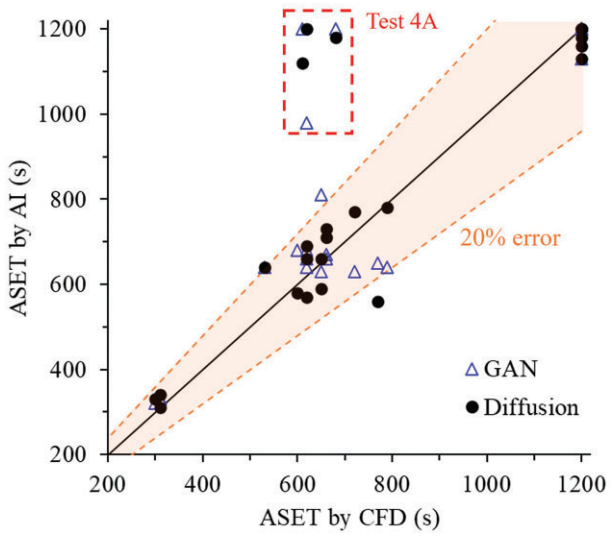

Figure 10: ASET comparison for testing cases.

can be leveraged to enhance future schemes, fostering continuous improvement in fire safety and design practices.

Table 2 summarizes the features of three computation methods (CFD, GAN, and diffusion model). The traditional CFD model can provide high-fidelity smoke flow results and detailed patterns for the whole building space, but it is costly in terms of both computational time consumption and required resources such as a dedicated server. The GAN model offers a prompt prediction of smoke flow in the order of seconds for a typical 1200-s fire-smoke analysis, which can be performed on any computer with a CPU. Although GAN model ignores many details and patterns of smoke flow in generated images, it can still determine the general

Table 2: Features of three computational methods for PBD of building fire safety.

Features	CFD model	GAN model	Diffusion model
Model training time	–	Days	Weeks
Cost for typical fire analysis	Weeks (PC) days (server)	Seconds (CPU)	Days (CPU), hours (GPU)
Applicable design stage	Later phase	Whole stages	Whole stages
Usage of past data	One-time	Learn patterns for new cases	Learn patterns for new cases
Smoke image quality	Ground truth	General tendency	Smoke pattern details
2-m Visibility accuracy	Ground truth	85% and 90% (w/o Test 4A)	87% and 92% (w/o Test 4A)

tendency of the smoke layer development, in order to satisfy the engineering practices of ASET estimation.

On the other hand, the required computational cost for the diffusion model is more than that of the GAN model but still much less than that of the CFD model. For example, a GPU is usually required for model training and smoke image rendering. Although it can generate smoke images with more smoke pattern details, it has no significant improvement in the prediction accuracy in terms of 2-m visibility profile or ASET value. Therefore, the GAN model might be a better solution for future development of the AI-PBD method unless there is a technical improvement that can significantly reduce the rendering time of the diffusion model. Nevertheless, the diffusion model shows its great potential for tasks requiring smoke pattern details and good visualization.

With reduced computational cost, the application of fire engineering analysis has expanded from the later stages of design to the early conceptual design phase via AI methods. It allows for quick feedback on the design performance of fire safety, enabling designers to iterate and refine their designs more efficiently without worrying about later design changes due to unsatisfactory fire safety requirements. Moreover, faster calculations also allow for comprehensive parametric studies of the proposed design, e.g., effectiveness of the smoke extraction system. With low-cost AI predictions, engineers can quickly identify the optimal solutions. Finally, the past design data can be well inherited by the AI models and applied to similar future cases, which can avoid many repetitive design workloads and achieve automatic design.

Although this work demonstrates a great potential of AI in facilitating fire engineering design, there are still some limitations that need to be addressed to meet practical demands. Firstly, smoke movement behavior in atriums is influenced by various parameters other than just the atrium shape. As design inputs, factors such as smoke ventilation capacity, air makeup distribution, fuel properties, and customized HRR curves should be further considered. Nevertheless, these variables can be easily accounted for by expanding the training database.

Secondly, the current work has not considered the internal structures within the atrium, which are common in realistic indoor spaces, such as surrounding cloisters, core tubes, and smoke barriers. These structures can potentially impact smoke flow behaviors when their dimensions are sufficiently large (Zeng, Zhang, *et al.*, 2022). To address this challenge, upgrades to the data processing method and AI architecture should be implemented in addition to expanding the database. By addressing these limitations, the AI model can provide more comprehensive and accurate predictions, catering to the practical requirements of fire engineering design.

Lastly, given the data-driven nature of the AI, its flaw has also been demonstrated by introducing the distinct case in this study. The boundaries and limitations of the database and AI model must be fully recognized before using the synthesized results in the specific case.

4. Conclusions

This study develops AI models to provide accurate and prompt predictions on smoke movement in atriums with complex shapes. Initially, a numerical fire database was constructed, containing data on smoke layer development in various building geometries. This database was then utilized to train two AI models using the pix2pix GAN architecture and image-prompt diffusion model. By inputting information on the building shape and fire location, the proposed GAN models can deliver three soot visibility slices from the X, Y, and Z directions in a few seconds, with an average discrepancy of 15% for a new atrium that is not significantly distinct from the training cases. The diffusion model can reproduce more flow details and local smoke patterns but with a longer rendering time of 20 min.

These AI predictions can be further utilized to estimate the ASET by referring to the smoke descending profiles with an accuracy of 85% and up to 92% by excluding distinct case. In comparison to traditional methods based on CFD modeling, the AI-driven intelligent approach improves design efficiency, reduces computational costs, and creates a sustainable design environment. It enables engineers to conduct more comprehensive evaluations of proposed designs and effortlessly identify the most cost-effective solutions, marking a significant step toward intelligent and automatic design transformation.

Conflict of interest statement

None declared.

Acknowledgments

This work is funded by the Hong Kong Research Grants Council Theme-based Research Scheme (T22-505/19-N) and the National Natural Science Foundation of China (No. 52238011).

Authors' Contribution

Y.Z.: Investigation, Methodology, Writing—original draft, and Formal analysis. **Z.Z.:** Methodology and Formal analysis. **T.Z.:** Investigation and Formal analysis. **X.H.:** Conceptualization, Supervision, Writing—review & editing, and Funding acquisition. **X.L.:** Supervision and Writing—review & editing.

Supplementary Data

Supplementary data are available at *JCDENG* online.

Appendix 1

Fig. A1 presents some examples of creating two fire scenarios for each design scheme. By changing the fire location or the atrium

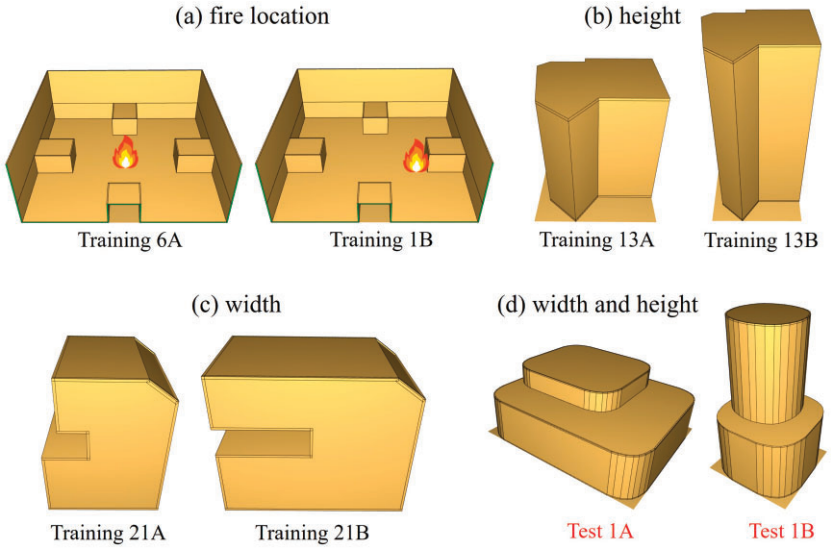

Figure A1: Examples of the database extension by changing (a) fire location; (b) building height; (c) building width; and (d) both building height and width.

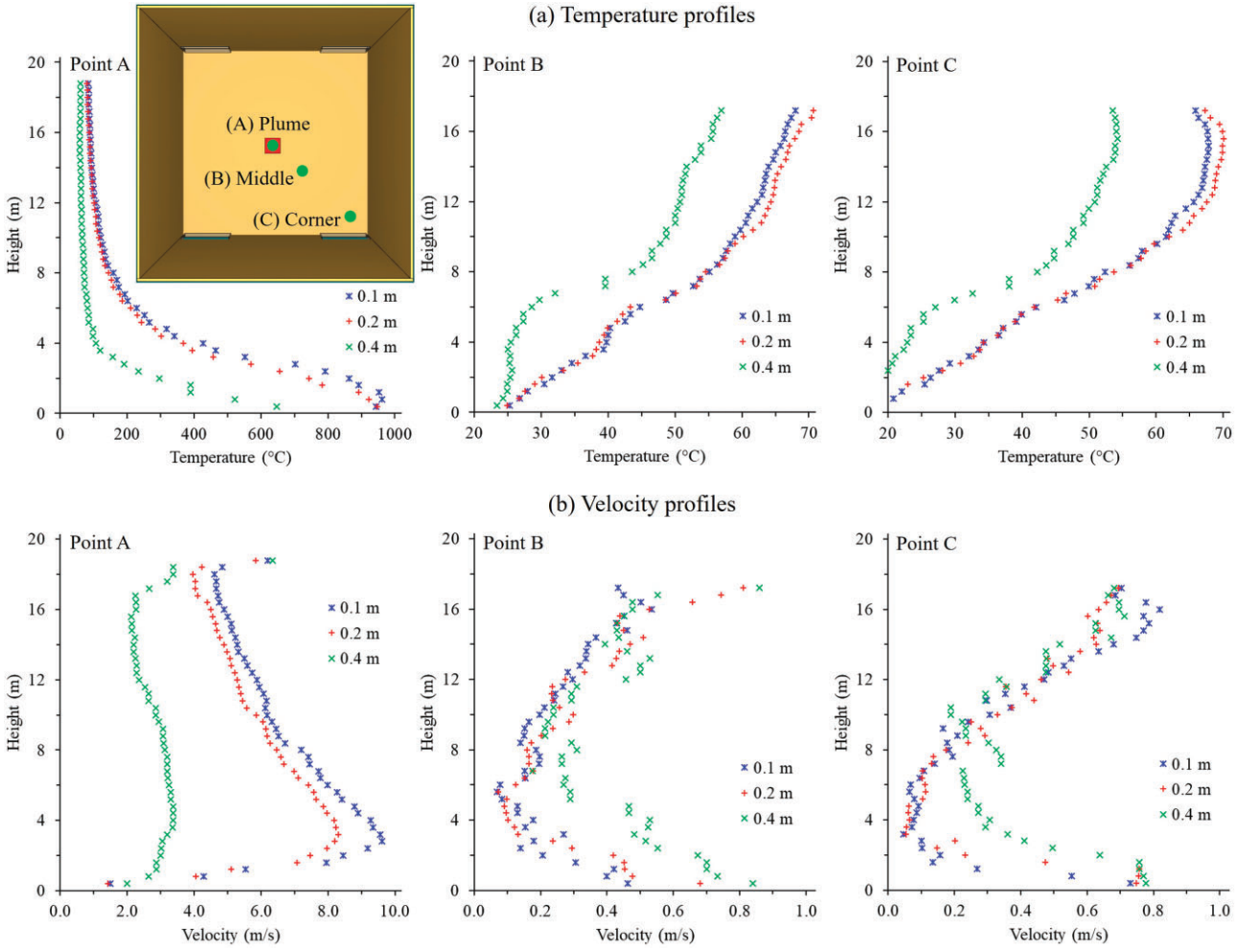

Figure A2: Grid sensitivity study on (a) temperature and (b) velocity profiles.

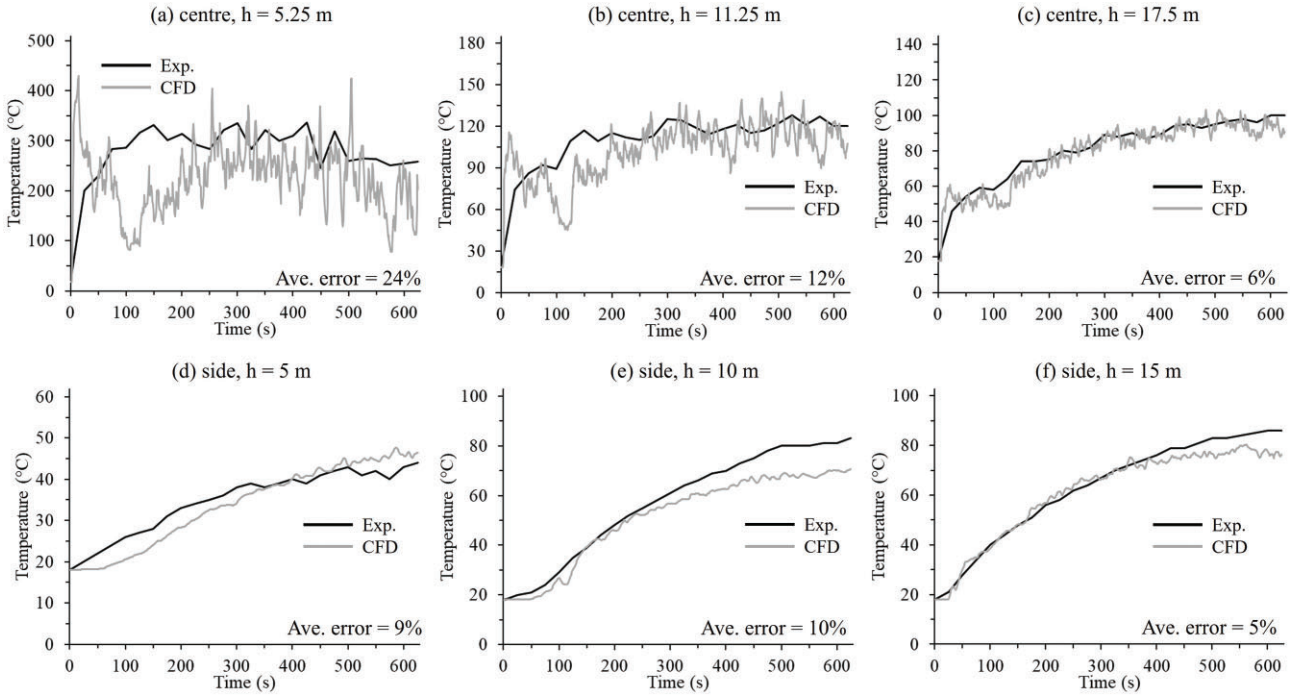

Figure A3: Temperature distribution of CFD fire model validated by a large atrium fire experiment (Ayala *et al.*, 2016).

dimension, e.g., building height or width, the size of the database can be doubled. Fig. A2 shows the result of grid sensitivity study, while the reduction of cell size from 0.2 to 0.1 m has no significant impacts on the gas temperature and velocity profiles at various arises. Fig. A3 shows the validation results of CFD model. The simulation results agree well with the experimental measurements. A small average discrepancy of 11% demonstrates the fidelity and creditability of the adopted CFD computational settings.

Data availability

The adopted training database is available on request.

References

Alpert, R. L. (1972). Calculation of response time of ceiling-mounted fire detectors. *Fire Technology*, **8**, 181–195. https://doi.org/10.1007/BF02590543.

Australian Building Codes Board. (2022). *Building code of Australia—Volume one*. Australian Building Codes Board.

Ayala, P., Cantizano, A., Rein, G., Vigne, G., & Gutiérrez-Montes, C. (2016). Fire experiments and simulations in a full-scale atrium under transient and asymmetric venting conditions. *Fire Technology*, **52**, 51–78. https://doi.org/10.1007/s10694-015-0487-9.

Bakas, I., & Kontoleon, K. J. (2021). Performance evaluation of artificial neural networks (ANN) predicting heat transfer through Masonry walls exposed to fire. *Applied Sciences*, **11**, 11435. https://doi.org/10.3390/app11231435.

Bakas, I., & Kontoleon, K. J. (2023). A review of the contributions of artificial intelligence in fire engineering, in a world rapidly realising the need for sustainable design. *IOP Conference Series: Earth and Environmental Science*, **1196**, 012112. https://doi.org/10.1088/1755-1315/1196/1/012112.

Building Department. (2011). *Code of practice for fire safety in buildings*. Building Department.

Cheung, W., Zeng, Y., Lin, S., & Huang, X. (2023) Modelling carbon monoxide transport and hazard from smouldering for building fire safety design analysis. *Fire Safety Journal*, **140**, 103895. https://doi.org/10.1016/j.firesaf.2023.103895.

China Railway Third Survey and Design Institute Group. (2016). *TB 10063-2016: Code for design of fire prevention for railway engineering*. China Railway Publishing House Limited Company.

Dhariwal, P., & Nichol, A. (2021). Diffusion models beat GANs on image synthesis. *Advances in Neural Information Processing Systems*, **11**, 8780–8794.

Fei, Y., Liao, W., Huang, Y., & Lu, X. (2022). Knowledge-enhanced generative adversarial networks for schematic design of framed tube structures. *Automation in Construction*, **144**, 104619. https://doi.org/10.1016/j.autcon.2022.104619.

Fei, Y., Liao, W., Lu, X., & Guan, H. (2024). Knowledge-enhanced graph neural networks for construction material quantity estimation of reinforced concrete buildings. *Computer-Aided Civil and Infrastructure Engineering*, **39**, 518–538. https://doi.org/10.1111/mice.13094.

Feng, Y., Fei, Y., Lin, Y., Liao, W., & Lu, X. (2023). Intelligent generative design for shear wall cross-sectional size using rule-embedded generative adversarial network. *Journal of Structural Engineering*, **149**, 1–14. https://doi.org/10.1061/JSENDH.STENG-12206.

Gu, Y., Huang, Y., Liao, W., & Lu, X. (2024). Intelligent design of shear wall layout based on diffusion models. *Computer-Aided Civil and Infrastructure Engineering*. https://doi.org/10.1111/mice.13236.

Heskestad, G. (1984). Engineering relations for fire plumes. *Fire Safety Journal*, **7**, 25–32. https://doi.org/10.1016/0379-7112(84)90005-5.

Ho, J., Jain, A., & Abbeel, P. (2020). Denoising diffusion probabilistic models. In *Advances in neural information processing systems (NeurIPS 2020)* (Vol. **33**, pp. 1–12). https://doi.org/10.48550/arXiv.2006.11239.

Huang, W., & Zheng, H. (2018). Architectural drawings recognition and generation through machine learning. In *Proceedings of the 38th Annual Conference of the Association for Computer Aided Design in Architecture (ACADIA)* (pp. 156–165). https://doi.org/10.52842/conf.acadia.2018.156.

Isola, P., Zhu, J. Y., Zhou, T., & Efros, A. A. (2017). Image-to-image translation with conditional adversarial networks. In *Proceedings of the 30th IEEE Conference on Computer Vision and Pattern Recognition (CVPR 2017)* (pp. 5967–5976). https://doi.org/10.1109/CVPR.2017.632.

Kawagoe, K., & Sekine, T. (1963). Estimation of fire temperature rise curves in concrete buildings and its application. *Bulletin of Japan Association for Fire Science and Engineering*, **13**, 1–12. https://doi.org/10.11196/kasai.13.1.

Khan, M. M., Tewarson, A., & Chaos, M. (2016). Combustion characteristics of materials and generation of fire products. In Hurley M. J. (Ed.), *SFPE handbook of fire protection engineering* (5th ed., pp. 1143–1232). Springer.

Liao, W., Huang, Y., Zheng, Z., & Lu, X. (2022). Intelligent generative structural design method for shear wall building based on "fused-text-image-to-image" generative adversarial networks. *Expert Systems with Applications*, **210**, 118530. https://doi.org/10.1016/j.eswa.2022.118530.

Liao, W., Lu, X., Fei, Y., Gu, Y., & Huang, Y. (2024). Generative AI design for building structures. *Automation in Construction*, **157**, 105187. https://doi.org/10.1016/j.autcon.2023.105187.

Liao, W., Lu, X., Huang, Y., Zheng, Z., & Lin, Y. (2021). Automated structural design of shear wall residential buildings using generative adversarial networks. *Automation in Construction*, **132**, 103931. https://doi.org/10.1016/j.autcon.2021.103931.

Liao, W., Wang, X., Fei, Y., Huang, Y., Xie, L., & Lu, X. (2023). Base-isolation design of shear wall structures using physics-rule-co-guided self-supervised generative adversarial networks. *Earthquake Engineering & Structural Dynamics*, **52**, 3281–3303. https://doi.org/10.1002/eqe.3862.

Lu, X., Liao, W., Zhang, Y., & Huang, Y. (2022). Intelligent structural design of shear wall residence using physics-enhanced generative adversarial networks. *Earthquake Engineering and Structural Dynamics*, **51**, 1657–1676. https://doi.org/10.1002/eqe.3632.

Luo, M., Zeng, Y., Su, L.-C., & Huang, X. (2024). Review and application of engineering design models for building fire smoke movement and control. *Emergency Management Science and Technology*, **4**, e001. https://doi.org/10.48130/emst-0024-0001.

McGrattan, K., Hostikka, S., McDermott, R., Floyd, J., & Vanella, M. (2019). Fire dynamics simulator user's guide. In *NIST special publication 1019* (6th ed.). National Institute of Standards and Technology. https://doi.org/10.6028/NIST.SP.1019.

McGrattan, K., Hostikka, S., McDermott, R., Floyd, J., Weinschenk, C., & Overholt, K. (2021). Fire dynamics simulator technical reference guide volume 3: Validation. In *NIST special publication 1018* (6th ed.). National Institute of Standards and Technology.

McGrattan, K., Hostikka, S., McDermott, R., Floyd, J., Weinschenk, C., & Overholt, K. (2023). Fire dynamics simulator technical reference guide volume 2: Verification. In *NIST special publication 1018-2* (6th ed.). National Institute of Standards and Technology.

New Zealand Centre for Advanced Engineering. (2008). Fire engineering design guide. In Spearpoint M. (Ed.), *Tribology international* (Vol. **11**, 3rd ed.). New Zealand Centre for Advanced Engineering. https://doi.org/10.1016/0301-679x(78)90024-5.

Nguyen, H. T. Q., Nguyen, K. T. Q., Le, T. C., & Zhang, G. (2021). Review on the use of artificial intelligence to predict fire performance of construction materials and their flame retardancy. *Molecules*, **26**, 1022. https://doi.org/10.3390/molecules26041022.

Su, L., Wu, X., Zhang, X., & Huang, X. (2021). Smart performance-based design for building fire safety: Prediction of smoke motion via AI. *Journal of Building Engineering*, **43**, 102529. https://doi.org/10.1016/j.jobe.2021.102529.

Tam, W. C., Fu, E. Y., Li, J., Huang, X., Chen, J., & Huang, M. X. (2022). A spatial temporal graph neural network model for predicting flashover in arbitrary building floorplans. *Engineering Applications of Artificial Intelligence*, **115**, 105258. https://doi.org/10.1016/j.engappai.2022.105258.

Wang, Z., Zhang, T., & Huang, X. (2023). Predicting real-time fire heat release rate by flame images and deep learning. *Proceedings of the Combustion Institute*, **39**, 4115–4123. https://doi.org/10.1016/j.proci.2022.07.062.

Wang, Z., Zhang, T., & Huang, X. (2024). Numerical modeling of compartment fires: Ventilation characteristics and limitation of Kawagoe's law. *Fire Technology*, **60**, 1245–1268. https://doi.org/10.1007/s10694-022-01218-1.

Wang, Z., Zhang, T., Wu, X., & Huang, X. (2022). Predicting transient building fire based on external smoke images and deep learning. *Journal of Building Engineering*, **47**, 103823. https://doi.org/10.1016/j.jobe.2021.103823.

Wong, K. H., & Wu, Y. (2024). Fire engineering analysis for complex geometry building based on BIM integrated simulation platform. In *Mechanisms and machine science* (Vol. **143**, pp. 1285–1295). Springer. https://doi.org/10.1007/978-3-031-42515-8_90.

Wu, X., Park, Y., Li, A., Huang, X., Xiao, F., & Usmani, A. (2021). Smart detection of fire source in tunnel based on the numerical database and artificial intelligence. *Fire Technology*, **57**, 657–682. https://doi.org/10.1007/s10694-020-00985-z.

Wu, X., Zhang, X., Huang, X., Xiao, F., & Usmani, A. (2022). A real-time forecast of tunnel fire based on numerical database and artificial intelligence. *Building Simulation*, **15**, 511–524. https://doi.org/10.1007/s12273-021-0775-x.

Zeng, Y., Hon-Leung Wong, K., & Chen, L. (2019). Numerical study of the performance of automatic sprinkler system in dense equipment room. In *Proceedings of the 2019 9th International Conference on Fire Science and Fire Protection Engineering (ICFSFPE)*. https://doi.org/10.1109/ICFSFPE48751.2019.9055794.

Zeng, Y., & Huang, X. (2024a). Artificial intelligence powered building fire safety design analysis. In Huang X., & Tam W. C. (Eds.), *Intelligent building fire safety and smart firefighting* (pp. 101–124). Springer. https://doi.org/10.1007/978-3-031-48161-1_5.

Zeng, Y., & Huang, X. (2024b). Smart building fire safety design driven by artificial intelligence. In Naser M. Z. (Ed.), *Interpretable machine learning for the analysis, design, assessment, and informed decision making for civil infrastructure* (pp. 111–133). Elsevier. https://doi.org/10.1016/B978-0-12-824073-1.00011-3.

Zeng, Y., Li, Y., Du, P., & Huang, X. (2023). Smart fire detection analysis in complex building floorplans powered by GAN. *Journal of Building Engineering*, **79**, 107858. https://doi.org/10.1016/j.jobe.2023.107858.

Zeng, Y., Wong, H. Y., Węgrzyński, W., & Huang, X. (2023). Revisiting Alpert's correlations: Numerical exploration of early-stage building fire and detection. *Fire Technology*, **59**, 2925–2948. https://doi.org/10.1007/s10694-023-01461-0.

Zeng, Y., Zhang, X., Su, L., Wu, X., & Xinyan, H. (2022). Artificial Intelligence tool for fire safety design (IFETool): Demonstration in large open spaces. *Case Studies in Thermal Engineering*, **40**, 102483. https://doi.org/10.1016/j.csite.2022.102483.

Zhang, T., Wang, Z., Wong, H. Y., Tam, W. C., Huang, X., & Xiao, F. (2022). Real-time forecast of compartment fire and flashover based on deep learning. *Fire Safety Journal*, **130**, 103579. https://doi.org/10.1016/j.firesaf.2022.103579.

Zhang, T., Wang, Z., Zeng, Y., Wu, X., Huang, X., & Xiao, F. (2022). Building Artificial-Intelligence Digital Fire (AID-Fire) system: A real-scale demonstration. *Journal of Building Engineering*, **62**, 105363. https://doi.org/10.1016/j.jobe.2022.105363.

Zhang, X., Wu, X., & Huang, X. (2022). Smart real-time forecast of transient tunnel fires by a dual-agent deep learning model. *Tunnelling and Underground Space Technology*, **129**, 104631. https://doi.org/10.1016/j.tust.2022.104631.

Zhao, P., Fei, Y., Huang, Y., Feng, Y., Liao, W., & Lu, X. (2023). Design-condition-informed shear wall layout design based on graph neural networks. *Advanced Engineering Informatics*, **58**, 102190. https://doi.org/10.1016/j.aei.2023.102190.

Zhao, P., Liao, W., Huang, Y., & Lu, X. (2023a). Intelligent beam layout design for frame structure based on graph neural networks. *Journal of Building Engineering*, **63**, 105499. https://doi.org/10.1016/j.jobe.2022.105499.

Zhao, P., Liao, W., Huang, Y., & Lu, X. (2023b). Intelligent design of shear wall layout based on attention-enhanced generative adversarial network. *Engineering Structures*, **274**, 115170. https://doi.org/10.1016/j.engstruct.2022.115170.

Zhao, P., Liao, W., Huang, Y., & Lu, X. (2024). Beam layout design of shear wall structures based on graph neural networks. *Automation in Construction*, **158**, 105223. https://doi.org/10.1016/j.autcon.2023.105223.

Zhao, P., Liao, W., Xue, H., & Lu, X. (2022). Intelligent design method for beam and slab of shear wall structure based on deep learning. *Journal of Building Engineering*, **57**, 104838. https://doi.org/10.1016/j.jobe.2022.104838.

Zheng, Y., Liu, Y., Ma, L., & Wong, H. K. (2022). Fire safety design strategy of special space at the top of super high-rise building. In *Advances in transdisciplinary engineering* (Vol. **31**, pp. 222–231). IOS Press. https://doi.org/10.3233/ATDE220871.

Zheng, Z., Zhou, Y.-C., Chen, K.-Y., Lu, X.-Z., She, Z.-T., & Lin, J.-R. (2024). A text classification-based approach for evaluating and enhancing the machine interpretability of building codes. *Engineering Applications of Artificial Intelligence*, **127**, 107207. https://doi.org/10.1016/j.engappai.2023.107207.

Zheng, Z., Zhou, Y., Lu, X., & Lin, J. (2022). Knowledge-informed semantic alignment and rule interpretation for automated compliance checking. *Automation in Construction*, **142**, 104524. https://doi.org/10.1016/j.autcon.2022.104524.

Received: April 6, 2024. **Revised:** May 27, 2024. **Accepted:** May 29, 2024